Electric-Field-Induced Modification of the Magnon Energy, Exchange Interaction, and Curie Temperature of Transition-Metal Thin Films

M. Oba, K. Nakamura, T. Akiyama, T. Ito, M. Weinert, and A. J. Freeman

Phys. Rev. Lett. **114**, 107202 — Published 13 March 2015

DOI: 10.1103/PhysRevLett.114.107202

Electric-Field-Induced Modification of Magnon Energy, Exchange Interaction, and Curie Temperature of Transition-Metal Thin Films

M. Oba,[1] K. Nakamura,[1,*] T. Akiyama,[1] T. Ito,[1] M. Weinert,[2] and A. J. Freeman[3]

[1]*Department of Physics Engineering, Mie University, Tsu, Mie 514-8507, Japan*

[2]*Department of Physics, University of Wisconsin-Milwaukee, Milwaukee, Wisconsin 53201*

[3]*Department of Physics and Astronomy, Northwestern University, Evanston, Illinois 60208*

(Dated: December 4, 2014)

Abstract

The electric-field-induced modification in the Curie temperature of prototypical transition-metal thin films with the perpendicular magnetic easy axis, a freestanding Fe(001) monolayer and a Co monolayer on Pt(111), is investigated by first-principles calculations of spin-spiral structures in an external electric field (E-field). An applied E-field is found to modify the magnon (spin-spiral formation) energy; the change arises from the E-field-induced screening charge density in the spin-spiral states due to p-d hybridizations. The Heisenberg exchange parameters obtained from the magnon energy suggest an E-field-induced modification of the Curie temperature, which is demonstrated via Monte Carlo simulations that take the magnetocrystalline anisotropy into account.

PACS numbers: 75.70.Ak, 71.20.Be, 73.20.At

Electric field (E-field) induced magnetism in itinerant transition-metals has shown promise as a potential approach offering a new pathway to control magnetism at the nano-scale with ultralow-energy power consumption. It was originally reported that the coercivity of thin films of FePt and FePd was reversibly varied by the application of a voltage [1]. Later, the magnetocrystalline anisotropy (MCA) of the $3d$ transition-metal thin films with MgO interfaces was successfully controlled by a voltage [2–6], thus opening a new avenue towards MgO-based magnetic tunnel junction electronics [6]. It is now agreed that a change in the screening charge density due to the E-field, which causes a small change in band structures around the Fermi energy ($E_{\rm F}$), gives rise to the modification of the MCA energy [7–10].

A continuing challenge is an E-field control of the Curie temperature, $T_{\rm C}$, of ferromagnets [11–18]. In diluted ferromagnetic semiconductors such as (Ga,Mn)As and (In,Mn)As, a modification in the carrier density by an applied voltage leads to a change in the $T_{\rm C}$ [11–13], but with the serious shortcoming that $T_{\rm C}$ is inevitably less than a room temperature. Recently, a small change ($\sim$12 K) in the $T_{\rm C}$ with an applied gate voltage was reported experimentally for metal thin Co films (4 Å) [15] where the $T_{\rm C}$ is around 300$\sim$330 K. Further, the very large E-field created by the electrolytic double layer formed by a polymer film containing an ionic liquid enhances the change in $T_{\rm C}$ up to about 100 K [16]. Similar behavior was also suggested for metal thin Fe films from electrolytic double layer experiments [17].

Theoretically, an E-field-induced $T_{\rm C}$ modification at metal surfaces was proposed based on the surface critical phenomena [19] and the change in the number of electrons, N, but the experimental observations for Co/Pt(111) [15, 16] that an increase of N (by a positive E-field) tends to increases $T_{\rm C}$ was opposite to the theoretical prediction [20]. In films with two-dimensional (2D) character, a change in the MCA with the perpendicular magnetic easy axis may further drive the $T_{\rm C}$ modification [21, 22]. However, an quantitative understanding of the underlying physics and the mechanism of the E-field-induced $T_{\rm C}$ modification is still lacking, which hinders a search for other promising thin film candidates.

Here, we demonstrate an E-field-induced $T_{\rm C}$ modification from first-principles calculations for prototypical transition-metal thin films with perpendicular magnetic easy axis, a freestanding Fe monolayer and a Co monolayer on Pt(111). The results predict that an applied E-field modifies the magnon (spin-spiral formation) energy compared to the zero

field value, leading to modification of the Heisenberg exchange parameters.

Calculations were performed using the full-potential linearized augmented plane-wave (FLAPW) method [23–25] that treats a film geometry by including fully the additional (non-periodic) vacuum regions outside of a single slab. This geometry allows the inclusion of an E-field along the surface normal with proper boundary conditions [8, 26]. For treating spin-spiral structures in an E-field, the generalized Bloch theorem[27, 28] is introduced into the FLAPW method [29, 30]. Self-consistent calculations were carried out in the scalar relativistic approximation based on the local spin density approximation (LSDA) [31] for the freestanding Fe monolayer and the generalized gradient approximation (GGA) [32] for the Co/Pt. LAPW functions with a cutoff of $|\mathbf{k}+\mathbf{G}| \leq \mathbf{3.9}$ a.u., muffin-tin (MT) sphere radii of 2.2 a.u. for the Fe and Co atoms and 2.4 a.u. for the Pt atom, and an angular momentum cutoff of ℓ=8 were used. The spin-orbit coupling (SOC), needed to obtain the MCA in an E-field, was included using the second variation method. The uses of 9,000 and 3600 special $\mathbf{k}$-points in the full two-dimensional Brilliouin zone (BZ) for the freestanding Fe monolayer and the Co/Pt(111), respectively, were confirmed to suppress numerical fluctuations in the spin-spiral formation energy.

For a simplicity in discussion, first, we present for the freestanding Fe monolayer with an in-plane lattice constant of MgO(001) in E-fields of zero and 1 V/Å. The applied E-fields, defined at vacuum region enough far from the surfaces, may be near the maximum expected fields attainable before the dielectric breakdown of high-κ gate insulators in devices [18] such as MgO (dielectric constant is 9.8) and HfO (20). The calculated magnon (spin-spiral formation) energy, $E(\mathbf{q})$, relative to the antiferromagnetic state as a function of the spiral wave vector, $\mathbf{q}$, along high-symmetry directions is shown in Fig. 1. In zero field, the $E(\mathbf{q})$ in the neighborhood of $\bar{\Gamma}$ increases approximately proportional to the square of $\mathbf{q}$, characteristic of a ferromagnet. We confirmed that there is almost no change in the magnetic moments ($\sim$3.2 μ_{B}) as $\mathbf{q}$ varies. When an E-field is applied, $E(\mathbf{q})$ shows the same trend as in zero field, but an E-field-induced modification in $E(\mathbf{q})$ is observed, e.g., along $\bar{\Gamma}$ to $\bar{\mathrm{M}}$ $E(\mathbf{q})$ is modified by a few meV/atom compared to zero field.

The density of states (DOS) for the spin spiral states with $\mathbf{q}$ along $\bar{\Gamma}$ to $\bar{\mathrm{M}}$ illustrate the E-field-induced modification of the band structures, as shown in Fig. 2 (a). In zero field, the DOS at $\bar{\Gamma}$ has a wide bandwidth due to its itinerant ferromagnetic behavior. When $\mathbf{q}$ increases, however, the bandwidth gradually narrows, since the electron hopping to the

neighboring atoms, where the spin-up and -down states do not mix, is suppressed due to the spin-spiral rotation. When an E-field is applied, two small pseudogaps below and above the $E_{\rm F}$ (arrows in the figure) appear at $\bar{\Gamma}$, originating from the screening charge density in the E-field, as pointed out previously [8]. An important trend can be further discerned: the pseudogaps have a noticeable variation with respect to $\mathbf{q}$, and tend to disappear when $\mathbf{q}$ is close to $\bar{\rm M}$. Thus, the screening charge density behaves differently depending on $\mathbf{q}$, leading to the modification in the magnon dispersion (c.f., Fig. 1).

To get a clearer understanding of such screening behavior, the partial DOS projected onto the p_z and d_{z^2} orbitals are presented in Figs. 2 (b) and (c). In zero field, the p_z and d_{z^2} states at $\bar{\Gamma}$ extend widely above and below $E_{\rm F}$. However, the application of an E-field causes a p-d hybridization that induces the pseudogap above $E_{\rm F}$. The pseudogap below $E_{\rm F}$ in Fig. 2 (a) was confirmed to arise mainly from $p_{x,y}$-$d_{xz,yz}$ hybridization. As pointed out previously [8], an E-field at an atomic site is described by the Y_0^1 spherical harmonic, which couples orbitals with ℓ and $\ell \pm 1$ (e.g., p and d orbitals) and the same magnetic quantum number m. Indeed, the p_z ($m = 0$) orbitals couple to the d_{z^2} states, inducing an energy gap. Similarly, the $p_{x,y}$ ($m = \pm 1$) orbitals couple to the $d_{xz,yz}$ states. As $\mathbf{q}$ moves away from $\bar{\Gamma}$, the bandwidths of the p and d orbitals narrow, and the p states shift down in energy below $E_{\rm F}$ while the d states shift up above $E_{\rm F}$, decreasing the p-d hybridization.

The exchange parameters for zero and 1 V/Å within the classical Heisenberg model, $\mathcal{H} = \sum_{i<j} J_{ij} \mathbf{e}_i \cdot \mathbf{e}_j$, obtained by back Fourier transforming the magnon energy [33, 34], are shown in Fig. 3 (a). (The J_{ij} are extracted from the $E(\mathbf{q})$ given on an uniform 10×10 $\mathbf{q}$-points in the first BZ.) In zero field, the nearest-neighbor exchange parameter (J_{01}) has a positive value which stabilizes parallel alignment between the nearest-neighbor atomic moments; for the third-neighbors (J_{03}), an antiparallel coupling is favorable. When an E-field is applied, J_{01} increases by 0.5 meV compared to that in zero field, which enhances the ordering of the parallel magnetic moment alignment, but for the third nearest neighbors, the J_{03} decreases by 0.3 meV, which tends to favor the antiparallel alignment. The difference in the integrated exchange interaction energy, $\sum_j J_{0j}(1{\rm V/Å}) - \sum_j J_{0j}(0{\rm V/Å})$, is 1.5 meV, which suggests that the applied E-field increases $T_{\rm C}$, by 11 K within mean-field theory (MFT).

The Heisenberg exchange parameters are, however, unsatisfactory for a 2D ferromagnet such as the present Fe monolayer, since according to the Mermin-Wagner theorem [35] the

isotropic Heisenberg ferromagnet cannot order above zero temperature. A perpendicular MCA, however, is known to stabilize long-rage ferromagnetic order at finite temperatures by introducing an anisotropy-induced gap at the bottom of the spin wave spectrum [21, 22]. Since calculations with SOC are restricted to commensurate spin spiral states [29], we simply included the MCA energy, $\mathcal{H}_{\rm MCA} = \sum_i K \mathbf{e}_{z,i}^2$, where K is a MCA parameter, in Monte Carlo simulations [36] with a 70×70 square-lattice cell to estimate $T_{\rm C}$. As shown in Fig. 3 (b), $T_{\rm C}$ varies significantly with K, with $T_{\rm C}$ decreasing to zero as K approaches zero, in agreement with the Mermin-Wagner theorem [35], while the modification of $T_{\rm C}$ due to the change in the exchange interaction is small. Since K of the freestanding Fe monolayer changes from 0.2 meV/atom to almost zero when an E-field of 1 V/Å is applied [8], the $T_{\rm C}$ modification is governed by the change in the MCA, where $T_{\rm C}$ decreases when K decreases.

We now consider a Co monolayer on Pt(111) in E-fields of -0.5 and 0.5 V/Å. The Pt(111) was modeled by a three-atomic-layer slab and the Co atoms are located on hcp sites of the Pt(111) surface, as shown in an inset in Fig. 4, as in calculations for Co adsorption on the Pt(111) surface [38]. The Co and top Pt layers were allowed to fully relax using the atomic forces while the lower two Pt layers are fixed in the positions to the calculated bulk value. Almost no relaxation caused by the E-fields is observed, the distance between the Co and top Pt layers were altered by less than 0.2 % for both E-fields compared to that in zero field.

The calculated $E(\mathbf{q})$ is presented in Fig. 4, where $E(\mathbf{q})$ shows ferromagnetic characteristics. Although $E(\mathbf{q})$ in both E-fields have the same trend with variations of $\mathbf{q}$, the E-field-induced modification is clearly observed due to the different screening behavior of the charge density in the spiral wave states, as also seen in the freestanding Fe monolayer. The energy difference between the ferromagnetic ($\bar{\Gamma}$) and antiferromagnetic ($\bar{\rm K}$) states increases by 11.0 meV/Co-atom when the applied E-field is varied from -0.5 V/Å to 0.5 V/Å; this stabilizes the ferromagnetic ordering and so increases the exchange interaction of the J_{01} and J_{03} by 1.1 and 0.8 meV, respectively, as shown in Fig.5 (a). The difference in the integrated exchange interaction energy, $\sum_j J_{0j}(0.5{\rm V/Å}) - \sum_j J_{0j}(-0.5{\rm V/Å})$, is 10.3 meV, which suggests that the positive E-field increases $T_{\rm C}$ compared to that in a negative field, by 80 K in MFT.

The MCA energy, as calculated using the FLAPW method with SOC, results in K=0.50 and 0.10 meV/atom for -0.5 and 0.5 V/Å, respectively, where the magnetization energet-

ically favors orienting along the perpendicular direction. The positive (negative) E-field decreases (increases) the MCA energy, in agreement with experiments [39]. As discussed for the freestanding Fe monolayer, if $T_{\rm C}$ is governed by the MCA, $T_{\rm C}$ will decrease when the positive E-field is applied, but this trend is opposite to experimental observations [15, 16].

Taking K into account, Monte Carlo simulations with a 70×70 triangular-lattice cell were carried out. The magnetization, $M/M_{\rm S}$, as a function of the temperature T, are shown in Fig. 5 (b). The results clearly demonstrate that $T_{\rm C}$ for positive E-fields is higher than that in negative fields, by about 20 K, in agreement with experiments [15]. The calculated critical exponent is about 0.26 for both E-fields; the value gets roughly closer to experimental one [15]. The quantitative discrepancy to the experimental $T_{\rm C}$ of ∼320 K [15, 16] may be attributed to the simplicity in the present model, e.g., an ideal interface without defects such as inter-atomic mixing and roughness, but these effects will not alter the conclusions regarding the E-field dependence.

Finally, we comment on the relationship of between a change in the number of electrons (N) and the modification of $T_{\rm C}$. In the present calculations, the positive E-field (0.5 V/Å) increases N of the Co atom by 3.8 $\times 10^{-3}$ electrons compared to that in the negative E-field (-0.5 V/Å), as would naturally be expected. However, the number of the d electrons decreases by 1.1 $\times 10^{-3}$ electrons while the sp electrons increase by 4.5 $\times 10^{-3}$electrons, since the later electrons predominately contribute the screening of the E-field. The relation between the number of d elections and $T_{\rm C}$ behaves like the Slater-Pauling curve for $3d$ magnetic alloys [20], where when the valence d electrons decrease as $T_{\rm C}$ increases.

In summary, we investigated the electric field modification of $T_{\rm C}$ of a freestanding Fe monolayer and a Co monolayer on Pt(111) based on first-principles calculations that treat spin-spiral structures in an applied E-field. Our results predict that the calculated magnon (spin-spiral formation) energy in the presence of the E-field is modified by more than several meV compared to zero field. The Heisenberg exchange parameters obtained from the calculated magnon energies suggest that $T_{\rm C}$ will be modified by an E-field, a conclusion supported by Monte Carlo simulations that take the MCA into account.

We thank Prof. T. Oguchi and Prof. K. Sano for fruitful discussions. Work at Mie University was supported by a Grant-in-Aid for Scientific Research No. 20540334 from the Japan Society for the Promotion of Science, and the Cooperative Research Program of "Network Joint Research Center for Materials and Devices". Computations were performed

at Center for Computational Materials Science, Institute for Materials Research, Tohoku University, and Supercomputer Center, Institute for Solid State Physics, University of Tokyo. Work at Northwestern University was supported by the US Department of Energy DE-FG02-05ER45372. Work at University of Wisconsin-Milwaukee was supported by NSF DMR-1335215.

---

* Email address: kohji@phen.mie-u.ac.jp

[1] M. Weisheit, S. Fähler, A. Marty, Y. Souche, C. Poinshignon, and D. Givord, Science **315**, 349 (2007).

[2] T. Maruyama, K. Ohta, T. Nozaki, T. Shinjo, M. Shiraishi, S. Mizukami, Y. Ando, and Y. Suzuki, Nature Nanotech. **4**, 158 (2009).

[3] K. Ohta, T. Maruyama, T. Nozaki, M. Shiraishi, T. Shinjo, Y. Suzuki, S.-S. Ha, C.-Y. You, and W. van Roy, Appl. Phys. Lett. **94**, 032501 (2009).

[4] Y. Shita, T Maruyama, T. Nozaki, T. Shinjyo, M. Shiraishi, and Y. Suzuki, Appl. Phys. Express **2**, 063001 (2009).

[5] M. Endo, S. Kanai, S. Ikeda, F. Matsukura, and H. Ohno, Appl. Phys. Lett. **96**, 212503 (2010).

[6] W.-G. Wang, M. Li, S. Hageman, and C. L. Chien, Nature Mater. **11**, 64 (2012).

[7] C.-G. Duan, J. P. Velev, R. F. Sabirianov, Z. Zhu, J. Chu, S. S. Jaswal, and E. Y. Tsymbal, Phys. Rev. Lett. **101**, 137201 (2008).

[8] K. Nakamura, R. Shimabukuro, Y. Fujiwara, T. Akiyama, T. Ito, and A. J. Freeman, Phys. Rev. Lett. **102**, 187201 (2009).

[9] M. Tsujikawa and T. Oda, Phys. Rev. Lett. **102**, 247203 (2009).

[10] K. Nakamura, T. Akiyama, T. Ito, M. Weinert, and A. J. Freeman, Phys. Rev. B **81**, 220409 (2010).

[11] H. Ohno, D. Chiba, F. Matsukura, T. Omiya, E. Abe, T. Dietl, Y. Ohno, and K. Ohtani, Nature **408**, 944 (2000).

[12] H. Boukari, P. Kossacki, M. Bertolini, D. Ferrand, J. Cibert, S. Tatarenko, A. Wasiela, J. A. Gaj, and T. Dietl, Phys. Rev. Lett. **88**, 207204 (2002).

[13] D. Chiba, F. Matsukura, and H. Ohno, Appl. Phys. Lett. **89**, 162505 (2006).

[14] Y. Yamada, K. Ueno, T. Fukumura, H. T. Yuan, H. Shimotani, Y. Iwasa, L. Gu, S. Tsukimoto, Y. Ikuhara, M. Kawasaki, Science **332**, 1065 (2011).

[15] D. Chiba, S. Fukami, K. Shimamura, N. Ishiwata, K. Kobayashi, and T. Ono, Nature Mater. **10**, 853 (2011).

[16] K. Shimamura, D. Chiba, S. Ono, S. Fukami, N. Ishiwata, M. Kawaguchi, K. Kobayashi, and T. Ono, Appl. Phys. Lett. **100**, 122402 (2012).

[17] M. Kawaguchi, K. Shimamura, S. Ono, S. Fukami, F. Matsukura, H. Ohno, D. Chiba, and T. Ono, Appl. Phys. Express **5**, 063007 (2012).

[18] D. Chiba and T. Ono, J. Phys. D: Appl. Phys. **46**, 213001 (2013).

[19] I. V. Ovchinnikov and K. L. Wang, Phys. Rev. B **79**, 020402R (2009).

[20] C. Takahashi, M. Ogura, and H. Akai, J. Phys.: Condens. Matter **19**, 365233 (2007).

[21] P. Bruno, Phys. Rev. B **43**, 6015 (1991).

[22] L. M. Sandratskii, E. Sasioglu, and P. Bruno, Phys. Rev. B **73**, 014430 (2006).

[23] E. Wimmer, H. Krakauer, M. Weinert, and A. J. Freeman, Phys. Rev. B **24**, 864 (1981).

[24] M. Weinert, E. Wimmer, and A. J. Freeman, Phys. Rev. B **26**, 4571 (1982).

[25] K. Nakamura, T. Ito, A. J. Freeman, L. Zhong, and J. Fernandez-de-Castro, Phys. Rev. B **67**, 014420 (2003).

[26] M. Weinert, G. Schneider, R. Podloucky, and J. Redinger, J. Phys.: Condens. Matter **21**, 084201 (2009).

[27] C. Herring, in *Magnetism*, edited by G. Rado and H. Suhl (Academic, New York, 1966).

[28] L. M. Sandratskii, Adv. Phys. **47**, 91 (1998).

[29] K. Nakamura, N. Mizuno, T. Akiyama, T. Ito, and A. J. Freeman, J. Appl. Phys. **99**, 08N501 (2006).

[30] K. Nakamura, T. Akiyama, T. Ito, and A. J. Freeman, J. Appl. Phys. **105**, 07C304 (2009).

[31] U. von Barth and L. Hedin, J. Phys. C **5**, 1629 (1972).

[32] J. P. Perdew, K. Burke, and M. Ernzerhof, Phys. Rev. Lett. **77**, 3865 (1996).

[33] S. V. Halilov, H. Eschrig, A. Y. Perlov, and P. M. Oppeneer, Phys. Rev. B **58**, 293 (1998).

[34] L. M. Sandratskii and P. Bruno, Phys. Rev. B **66** 134435 (2002).

[35] N. D. Mermin and H. Wagner, Phys. Rev. Lett. **17**, 1133 (1966).

[36] D. P. Landau and K. Binder, *A Guide to Monte Carlo Simulations in Statistical Physics*, (Cambridge University Press, Cambridge, 2000).

[37] R. Shimabukuro, K. Nakamura, T. Akiyama, T. Ito, Physica E **42**, 1014 (2010).

[38] P. Blonski and J. Hafner, J. Phys.: Condens. Matter **21**, 426001 (2009).

[39] K.Yamada, K. Kakizaki, K. Shimamura, M. Kawaguchi, S. Fukami, N. Ishiwata, D. Chiba, and T. Ono, Appl. Phys. Express **6**, 073004 (2013).

FIGURES

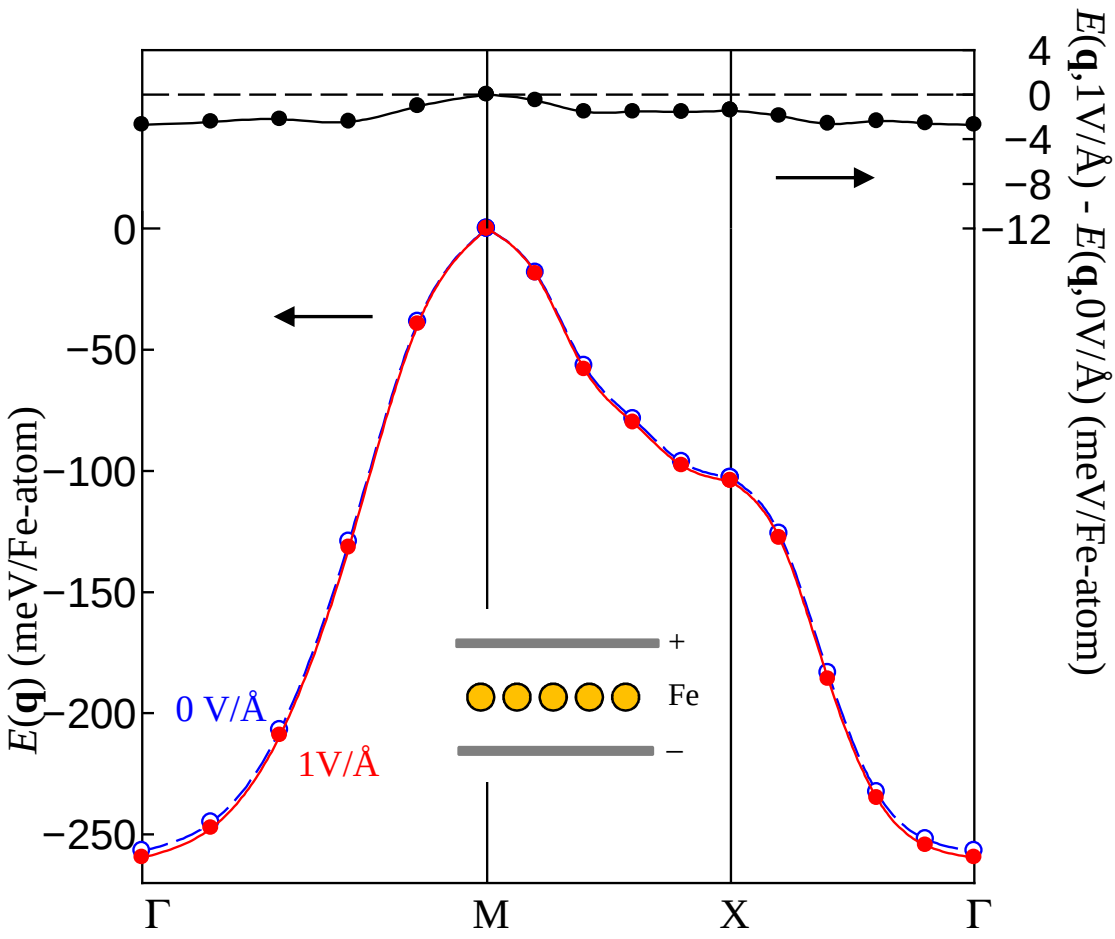

FIG. 1. (color online) Calculated magnon (spin-spiral formation) energy, $E(\mathbf{q})$, in E-fields of zero and 1 V/Å for an freestanding Fe monolayer as a function of the spiral wave vector, $\mathbf{q}$. The reference energy (E=0) is set to the value at $\bar{M}$ [$\mathbf{q}$=(0.5,0.5)] corresponding to an antiferromagnetic state, and open (blue) and solid (red) circles represent results at zero and 1 V/Å, respectively. Top in the figure shows the energy difference energy between zero and 1 V/Å. The inset shows a model of the monolayer in an E-field.

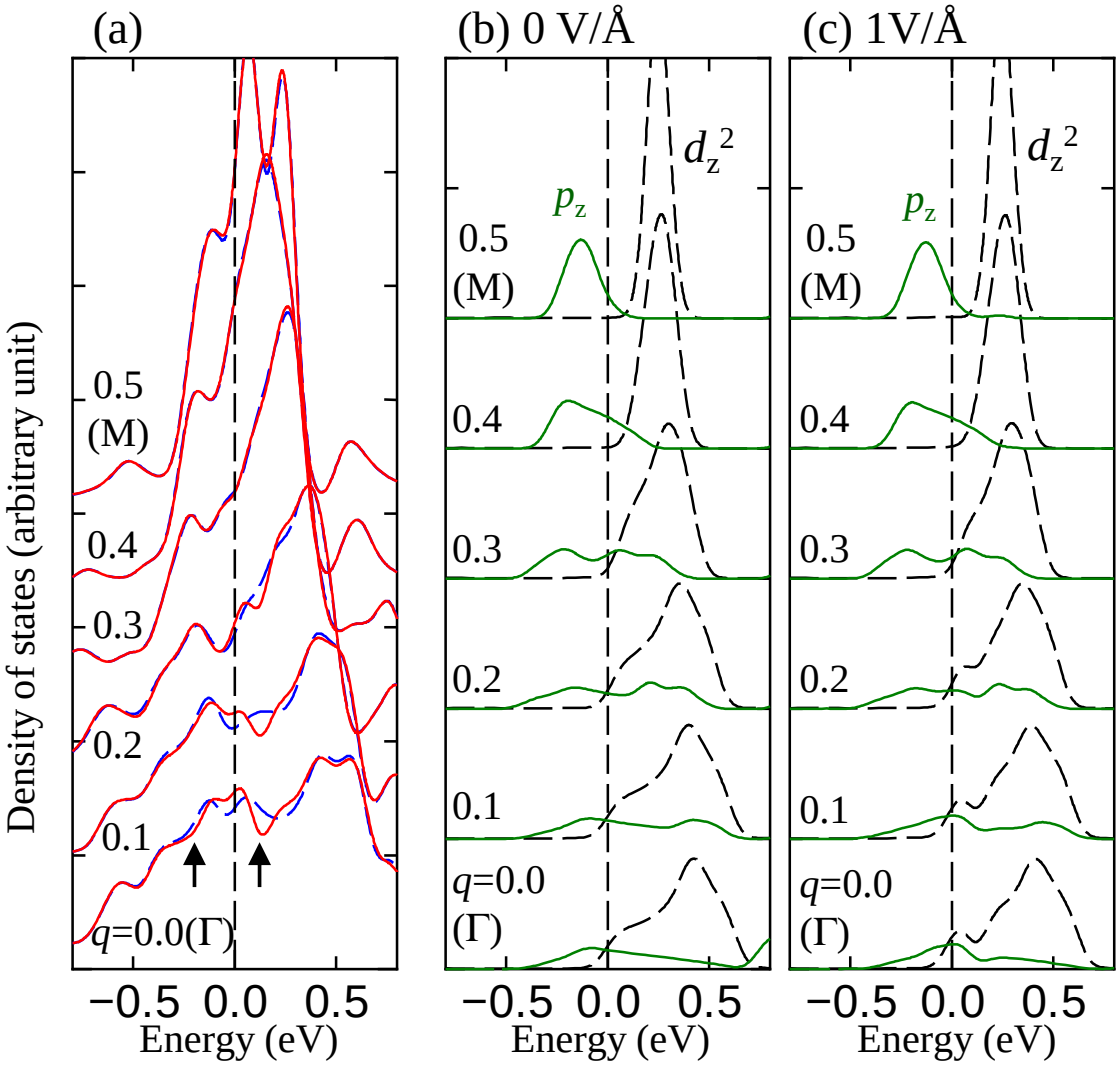

FIG. 2. (color online) (a) Calculated density of states (DOS) of an freestanding Fe monolayer at the spin wave vector $\mathbf{q}(q,q)$ from $\bar{\Gamma}$ [$\mathbf{q}$=(0,0) to $\bar{\mathrm{M}}$ [(0.5,0.5)]. Broken (blue) and solid (red) lines represent the DOS in zero and 1 V/Å of E-field, respectively, and the Fermi energy is set to zero. Arrows indicate pseudogaps induced by the E-field. (b) and (c) Partial DOS projected to the p_z (green solid lines) and d_{z^2} (black broken lines) orbitals in zero and 1 V/Å; the p_z DOS is magnified by 40 times with respect to the d_{z^2} DOS.

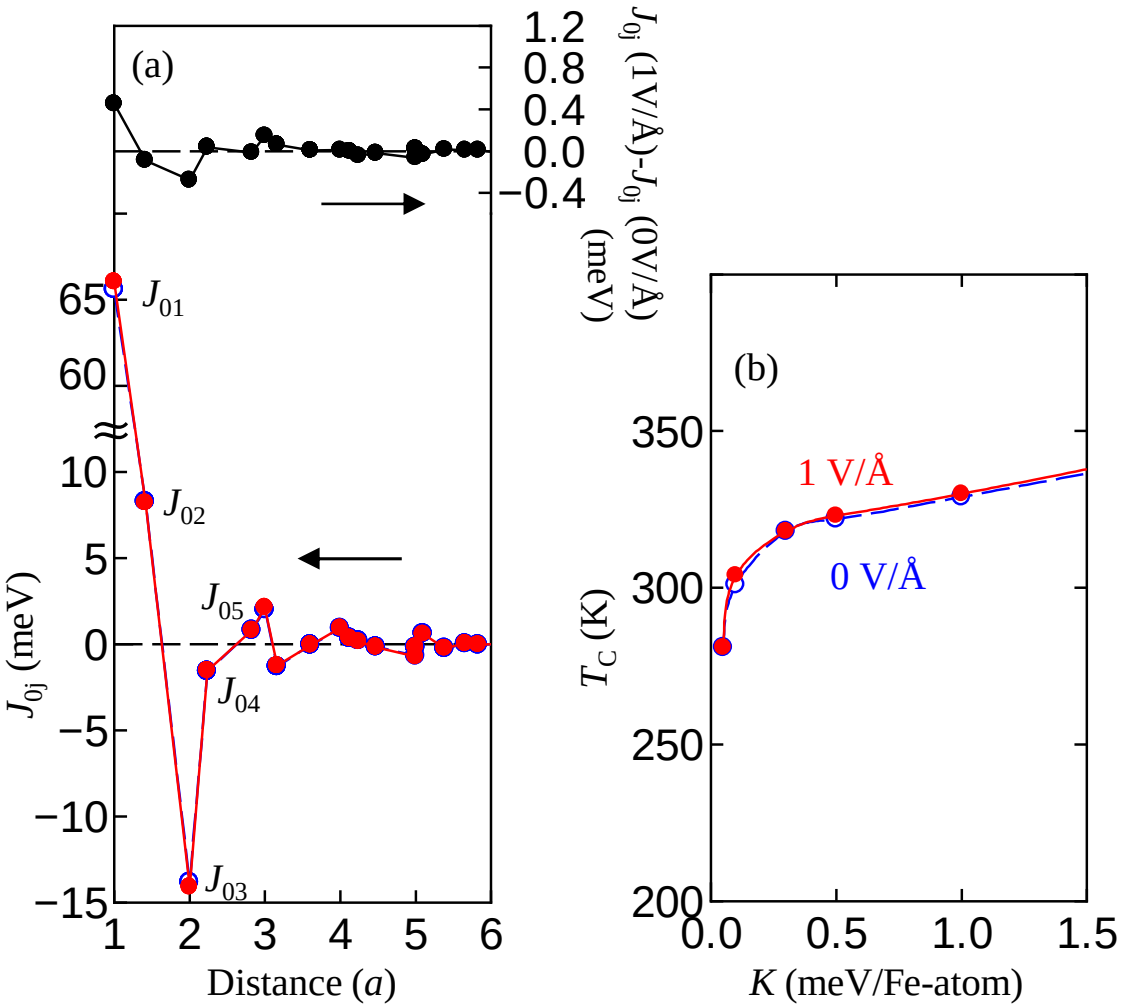

FIG. 3. (a) Calculated exchange parameters, J_{0i}, for an freestanding Fe monolayer obtained from back Fourier transforming the magnon energy, where the top curve shows the difference between zero and 1 V/Å. (b) Curie Temperature, $T_{\rm C}$, as a function of the magnetocrystalline anisotropy parameter, K, obtained by Monte Carlo simulations. Open (blue) and solid (red) circles indicate results for E-fields of zero and 1 V/Å, respectively.

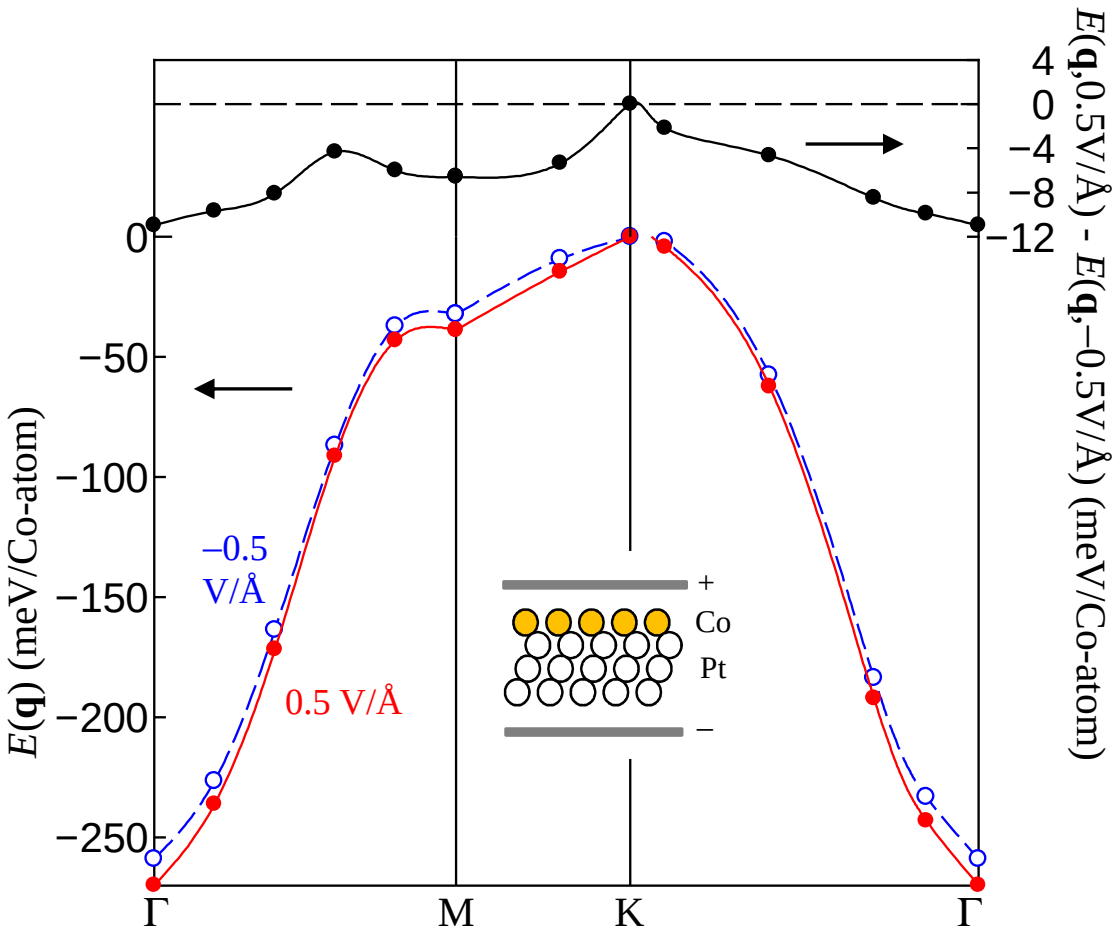

FIG. 4. Calculated magnon (spin-spiral formation) energy, $E(\mathbf{q})$, in E-fields of -0.5 and 0.5 V/Å for a Co monolayer on Pt(111) as a function of the spiral wave vector, $\mathbf{q}$. The reference energy (E=0) is set to the value at $\bar{\mathrm{K}}$ corresponding to an antiferromagnetic state, and open (blue) and solid (red) circles represent results at -0.5 and 0.5 V/Å, respectively. Top curve shows the energy difference between -0.5 and 0.5 V/Å; the inset shows a model of the Co monolayer on Pt(111) in a positive E-field.

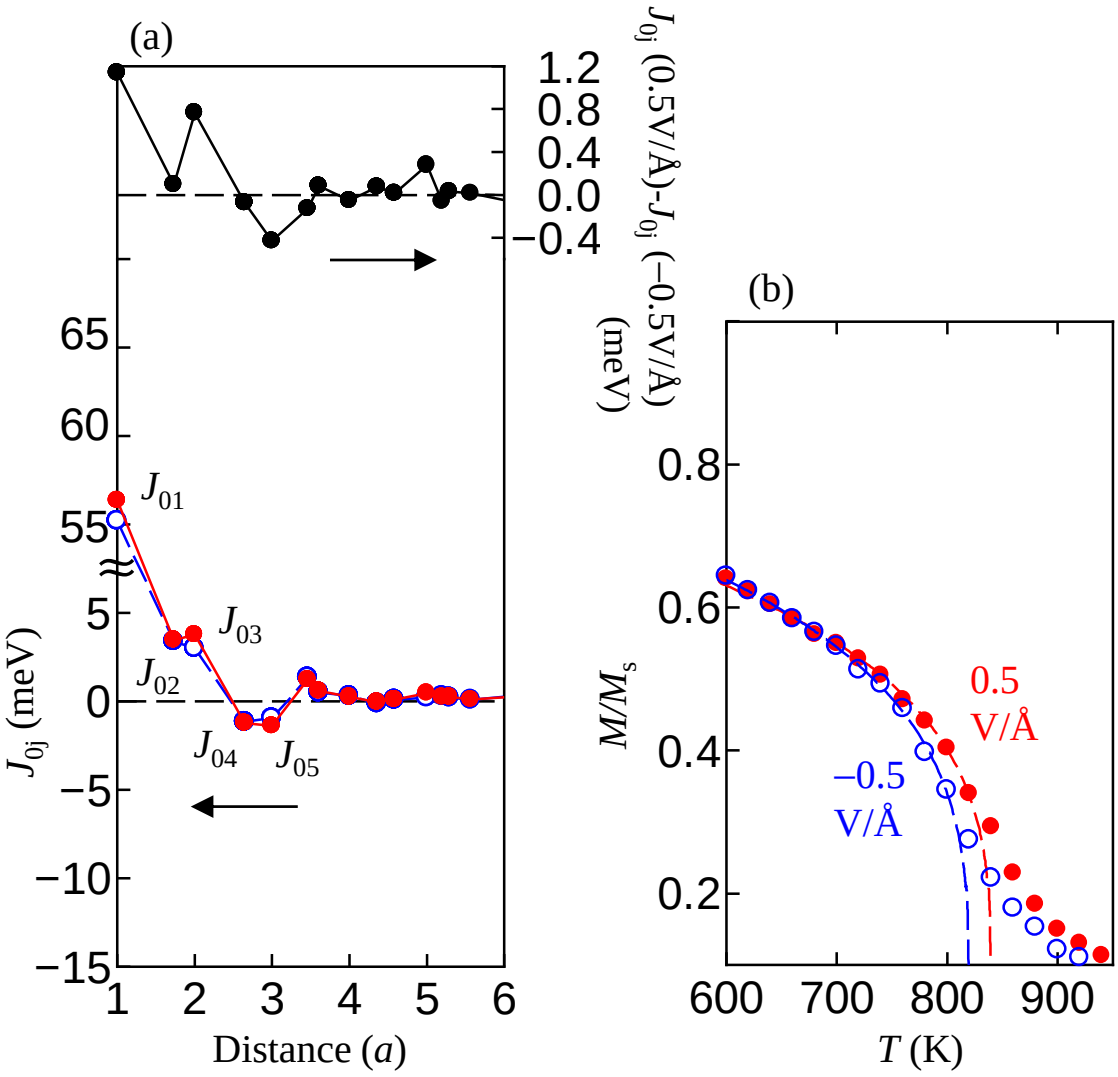

FIG. 5. (a) Calculated exchange parameters, J_{0i}, for a Co monolayer on Pt(111) in E-fields of -0.5 and 0.5 V/Å; the top curve shows the difference between both E-fields. (b) Magnetization, M/M_S as a function of the temperature, T, obtained from Monte Carlo simulations. Open (blue) and solid (red) circles indicate results for -0.5 and 0.5 V/Å, respectively.